Inorganic Chemistry

Article

pubs.acs.org/IC

Water-Soluble Tb^{3+} and Eu^{3+} Complexes with Ionophilic (Ionically Tagged) Ligands as Fluorescence Imaging Probes

Julia R. Diniz,[†] José R. Correa,[†] Daniel de A. Moreira,[‡] Rafaela S. Fontenele,[†] Aline L. de Oliveira,[†] Patrícia V. Abdelnur,[§] José D. L. Dutra,[∥] Ricardo O. Freire,[∥] Marcelo O. Rodrigues,*[,‡] and Brenno A. D. Neto*[,†]

[†]Laboratory of Medicinal and Technological Chemistry and [‡]LIMA-Laboratório de Inorgânica e Materiais, University of Brasilia (IQ-UnB), Campus Universitário Darcy Ribeiro, CEP 70904970, P.O. Box 4478, Brasilia-DF, Brazil

[§]National Center for Agroenergy Research, Brazilian Enterprise for Agricultural Research, EMBRAPA Agroenergy, 3448-4246 Brasília-DF, Brazil

[∥]Pople Computational Chemistry Laboratory, Universidade Federal de Sergipe, 49100-000, São Cristóvão, Sergipe, Brazil

Supporting Information

ABSTRACT: This article describes a straightforward and simple synthesis of ionically tagged water-soluble Eu^{3+} and Tb^{3+} complexes (with ionophilic ligands) applied for bioimaging of invasive mammal cancer cells (MDA-MB-231). Use of the task-specific ionic liquid 1-methyl-3-carboxymethyl-imidazolium chloride (**MAI·Cl**) as the ionophilic ligand (ionically tagged) proved to be a simple, elegant, and efficient strategy to obtain highly fluorescent water-soluble Eu^{3+} (**EuMAI**) and Tb^{3+} (**TbMAI**) complexes. **TbMAI** showed an intense bright green fluorescence emission selectively staining endoplasmic reticulum of MDA-MB-231 cells.

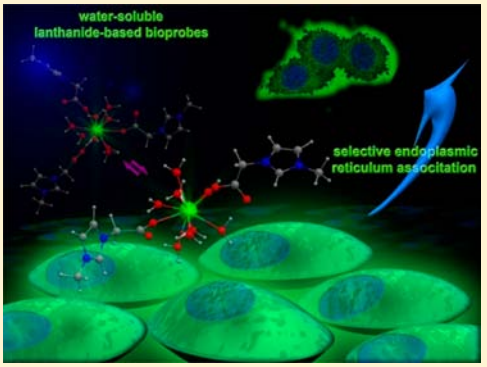

INTRODUCTION

Ionic liquids (ILs) and task-specific ionic liquids (TSILs) has become a reality for development of novel technologies and industrial application.[1] These ionic fluids are found widespread in many research and technological areas.[2−8] TSILs are commonly used, for instance, as organocatalysts, solvents, or ligands for metallic complexes which are usually applied as catalysts.[9−13] Due to their easily tunable properties, which are the net result of an appropriate combination of both cations and anions, the range of application for such materials is practically unlimited, especially for those based on the imidazolium cation.[14−16] It has been estimated that $\sim 10^6$ combinations of known cations and anions are capable of forming ILs (or TSILs),[17] thus making the reality of selecting and tuning a specific property for these ionic fluids virtually unlimited. Considering these features, some ligands have been tagged with imidazolium cations (also known as ionophilic ligands[18]) aiming to increase both their solubilities and affinities for a specific medium.[19−21] It is known that water miscibility (and with a plethora of organic solvents), polarity, viscosity, density, and other physicochemical properties can be fine tuned by tailoring a TSIL (or IL) with a suitable cation−anion combination.[22]

Bioimaging experiments are of paramount importance for biomedical, biological, and diagnostic technological growth and advance, as recently reviewed.[23] Today, there is huge interest on the search of novel lanthanide-based water-soluble luminescent bioprobes in order to improve the quality of bioimaging.[24−26] Their good characteristics encompass large Stoke shifts, narrow emission line spectra, long-wavelength emission, and long luminescence lifetimes; and have therefore brought fluorescent lanthanide-based probes to a prominent position.[27−29] Cellular membrane permeability is considered to be one of the most desired features for efficient bioimaging experiments.[30] To a broad range of biological assays, cellular membrane permeability is, indeed, the most important characteristic of a fluorogenic dye.[31] Fluorescent lanthanide complexes are highly sensitive fluorophores and usually capable of transposing the cell membrane.[32] In addition to all these attractive properties, lanthanide-based bioprobes have the advantage of low intrinsic cytotoxicity.[33,34] Despite all promising features observed for those bioprobes, it remains many drawbacks to be overcome. For instance, a straightforward synthesis of a water-soluble lanthanide bioprobe is among the most challenging tasks for development of this class of materials. Considering that lanthanide complexes are usually water insoluble,[35] it is more than reasonable to suggest that the use of ionophilic ligands bearing hydrophilic anions (e.g., chloride, bromide, iodide, and others) may be one of the best

Received: July 9, 2013
Published: August 14, 2013

   dx.doi.org/10.1021/ic4017678 | *Inorg. Chem.* 2013, 52, 10199−10205

strategies to overcome this major shortcoming, which currently narrows the biological application[36] of such promising class of materials.[37] Indeed, as already reviewed,[38−40] water solubility is a sine qua non condition toward an efficient lanthanide bioprobe development.

As expected, the combination of ILs and/or TSILs with fluorescent lanthanide-containing compounds has flourished with very promising results.[41] Typically, a substantial beneficial effect over the luminescent properties of lanthanide complexes is observed when doped with or dissolved in ILs (or TSILs), as recently reviewed.[42] Such ionic fluids (manly those based on the imidazolium cation) are known to be transparent through almost the whole visible and near-infrared spectral regions.[43] Moreover, these molten salts are capable of participating in the sensitization process of lanthanide complexes.[44] Somehow surprising, most reported studies describe the use of both ILs and TSILs as solvents or as the cationic moiety of the lanthanide-based structure (lanthanide metals as the anionic moieties) rather than ligands directly attached to the metal center. The use of ionophilic ligands directly attached to the lanthanide metal is a strategy barely explored, despite it has been proved to be a very promising approach for formation of new luminescent ionogels.[45] Indeed, this can be regarded as the unexplored world of task-specific ionic liquids, i.e., their use as ionophilic ligands for novel fluorescent water-soluble lanthanide complexes.

In this context, it is reasonable to envisage the combination of a TSIL (as the ionophilic ligand with hydrophilic anions) with lanthanides to afford new fluorescent water-soluble complexes. Hopefully, those new complexes may have their physicochemical properties fine tuned and influenced by the presence of the ionic tag tethered to their structures (Scheme 1); therefore, good water solubility and chemical stability are expected, which are properties usually observed for imidazolium derivatives bearing hydrophilic anions.[46]

Scheme 1. Strategy Aiming at Synthesis of Water-Soluble Lanthanide Complexes Using Ionically-Tagged (Ionophilic) Ligands[a]

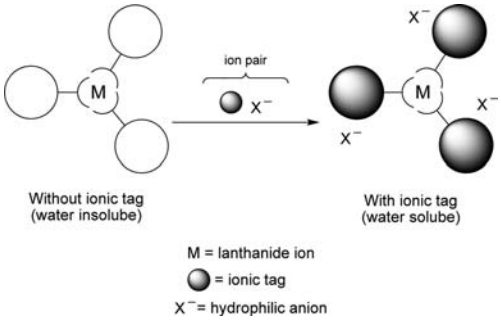

[a]Note that the ionic tag can be an imidazolium cation and the lanthanide complex (left) is usually water insoluble. Also note the anion (X^-) can be hydrophilic in order to facilitate the solubility in an aqueous medium.

Due to our interest in the development of novel fluorescent bioprobes[47−49] and in the chemistry and application of lanthanide-based compounds,[50−52] we present herein a probe design based on the use of a hydrophilic TSIL (1-methyl-3-carboxymethylimidazolium chloride, **MAI·Cl**) as the ionophilic ligand aiming at formation of new water-soluble fluorescent Eu^{3+} and Tb^{3+} complexes. These new lanthanide-based complexes were applied for cell-imaging experiments with invasive breast cancer cells lineage (MDA-MB-231).

RESULTS AND DISCUSSION

Initially, we synthesized two new Eu^{3+} and Tb^{3+} complexes (Scheme 2) using the known ionophilic ligand **MAI·Cl** that we

Scheme 2. Synthesis of Two Novel Water-Soluble Complexes (EuMAI and TbMAI) Using the Ionophilic Ligand MAI·Cl

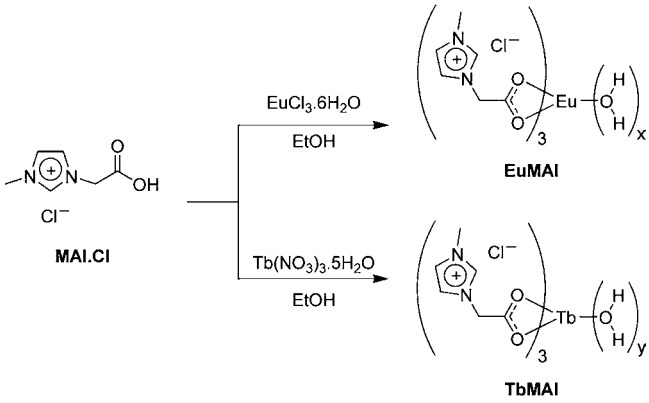

already used in the synthesis of Pd, Cu, and Ni complexes.[53] The two fluorescent lanthanides complexes, designated as **EuMAI** and **TbMAI**, were precipitated at pH 6.0 from ethanolic solutions containing a metal-to-ligand ratio of 1:3. Both complexes were shown to be totally water soluble at room temperature and highly hygroscopic in character.

As one could expect, the presence of the ionophilic ligands had a direct effect over the observed spectroscopic properties measured in aqueous solutions. Figure 1 exhibits the excitation spectra of **EuMAI** and **TbMAI** acquired at room temperature while monitoring the Eu^{3+} $^5D_0 \rightarrow {}^7F_2$ and Tb^{3+} $^5D_4 \rightarrow {}^7F_5$ transitions at 610 and 542 nm, respectively.

Spectra are dominated by a series of narrow peaks typical of 4f−4f transitions of the Ln^{3+} ions, indicating that direct excitation is the photophysical pathway responsible for the high luminescence of the samples. Steady-state emission spectra of **EuMAI** and **TbMAI** obtained in aqueous solutions are shown in Figure 2.

Spectra were composed of narrow bands characteristic of the Eu^{3+} $^5D_0 \rightarrow {}^7F_J$ transitions. Those attributed to the $^5D_0 \rightarrow {}^7F_2$ and $^5D_0 \rightarrow {}^7F_1$ transitions give the major contribution to **EuMAI** photoluminescence. It is well established that the Eu^{3+} $^5D_0 \rightarrow {}^7F_1$ transitions are governed by the magnetic dipole mechanism, hence, largely independent of the coordination sphere. However, the Eu^{3+} $^5D_0 \rightarrow {}^7F_2$ emission band, which is allowed by the electric dipole mechanism, is extremely sensitive to the symmetry around the Ln^{3+} ion and therefore known as a *hypersensitive* transition. It has been established that the intensity ratio between $^5D_0 \rightarrow {}^7F_2$ and $^5D_0 \rightarrow {}^7F_1$ transitions can be used as an internal probe to depict the symmetry around the Eu^{3+} ions.[54] Europium complexes with a low symmetric coordination sphere, such as Eu(β-diketonates)$_3$, have shown $^5D_0 \rightarrow {}^7F_2/{}^5D_0 \rightarrow {}^7F_1$ ratios ranging from 8 to 12, whereas a ratio of 0.67 has been associated to centrosymmetric compounds.[55] **EuMAI** complex has a $^5D_0 \rightarrow {}^7F_2/{}^5D_0 \rightarrow {}^7F_1$ value of 1.20, indicating that the local environment associated with Eu^{3+} ions is found in high symmetry. It may be justified, in

dx.doi.org/10.1021/ic4017678 | Inorg. Chem. 2013, 52, 10199−10205

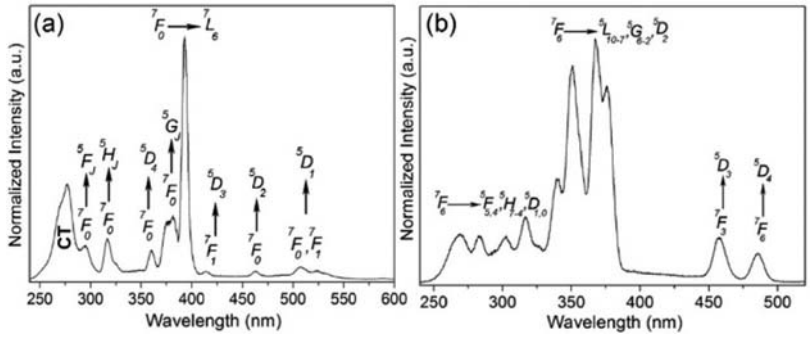

Figure 1. Excitation spectra of (a) **EuMAI** and (b) **TbMAI**. Aqueous solutions at 0.05 mmol.

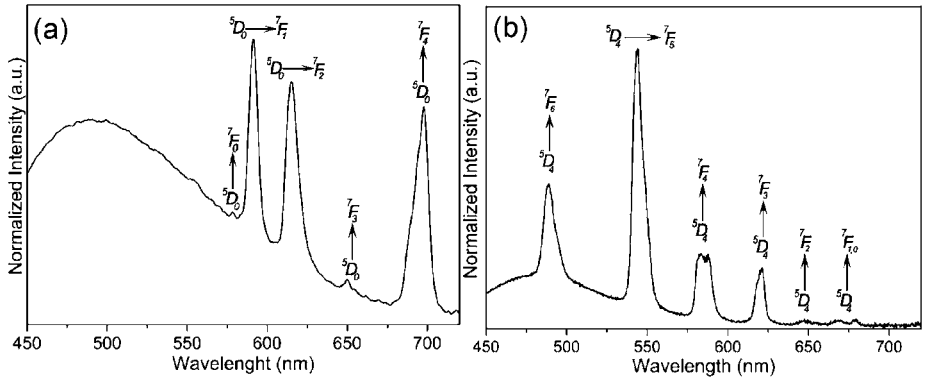

Figure 2. Emission spectra of (a) **EuMAI** and (b) **TbMAI**. Aqueous solutions at 0.05 mmol.

Scheme 3. EuMAI and TbMAI Equilibriums Observed in Aqueous Solutions

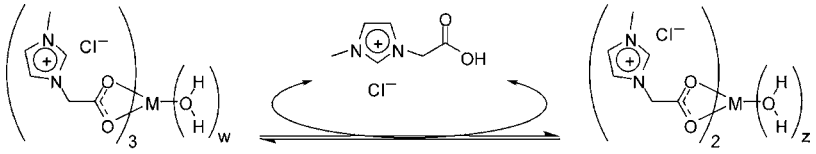

principle, by substitution of one **MAI** ligand for water molecules and the consequent conformational changes associated with ligand exchange. Although the emission spectrum of **EuMAI** displayed a typical profile of centrosymmetric complexes, it was possible to observe a peak centered at ca. 579 nm attributed to the $^5D_0 \rightarrow {}^7F_0$ transitions. The presence of the Eu^{3+} $^5D_0 \rightarrow {}^7F_0$ transitions indicated that the local symmetry around the Ln^{3+} ion is low and without an inversion center. Indeed, the selection rule for the electric dipole transition suggested that $^5D_0 \rightarrow {}^7F_0$ appears only if the point group of the Eu^{3+} ions is C_s, C_{nv}, or C_n.[56] These results demonstrated an equilibrium among distinct europium species in solution. To confirm this feature, NMR and electrospray (tandem) mass spectrometry (ESI-MS(/MS)) experiments were conducted. Photophysical data proved to be in good agreement with the data depicted from simple NMR analysis (see Supporting Information, Figures S1 and S2) and ESI(+)-MS(/MS) analyses (Figures S5−S8, Supporting Information). This equilibrium was also noted for the new Tb^{3+} complex (**TbMAI**), and Scheme 3 exemplifies this specific behavior.

ESI(+)-MS(/MS) was very efficient for detection and characterization of the metallic species (in equilibrium) found in solution. ESI-MS provides continuous snapshots of the ionic composition in solution,[57] and the obtained results reflect the dynamic equilibrium observed for both complexes (Scheme 3). By high-resolution ESI(+)-MS(/MS) it was possible to detect and characterize by collision-induced dissociation (structural diagnostic) the Ln^{3+} derivatives with two and three ligands in aqueous solution (Scheme 4). As observed for the NMR experiments, results from ESI-MS were also in accordance with the photophysical data. Interestingly, the Tb^{3+} derivatives were also detected and characterized with three H_2O molecules (see Figures S7 and S8, Supporting Information). It is worth noting that in all ESI-MS analyses there is a signal of m/z 141 attributed to the **MAI** cation, therefore pointing firmly to the proposed ligand dissociation/association equilibrium (Scheme 4) for both complexes.

Judd−Ofelt theory has been an important tool to calculate the spectroscopic properties of Eu^{3+} derivatives from their corrected emission spectra.[58,59] Following the described standard protocol,[60] the radiative decay rates from eq 1 were utilized to estimate the presence of water molecules coordinated to Eu^{3+} ions.[61] The number of water molecules coordinated to the metal center (n_w) was calculated from the phenomenological equation proposed by Supkowski and Horrocks (eq 1),[56,61,62] where A_{tot} (total decay rates) and A_{rad} (radiative rates) are expressed in ms^{-1} (Table 1).

dx.doi.org/10.1021/ic4017678 | Inorg. Chem. 2013, 52, 10199−10205

Scheme 4. Structures Detected and Characterized by High-Resolution ESI(+)-MS(/MS) in the Proposed Equilibriums[a]

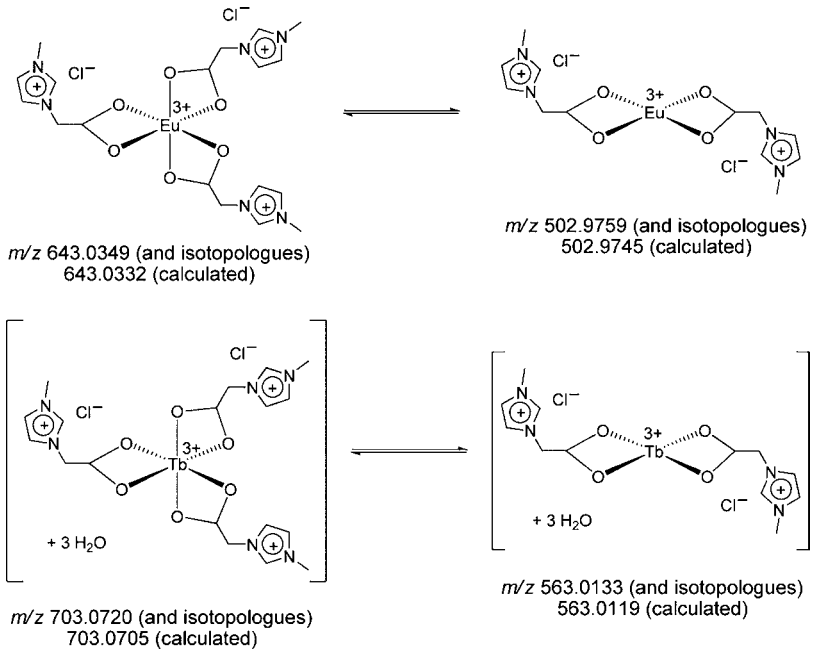

[a]Coordinated water molecules have been omitted in the metal coordination sphere for clarity. The ion of *m/z* 141 (free cation **MAI**) was also detected (see Figures S5–S8, Supporting Information) in accordance with the proposed equilibrium.

Table 1. Theoretical and Experimental Intensity Parameters Ω_2, Ω_4, and Ω_6, Radiative (A_{rad}) and Nonradiative (A_{nrad}) Decay Rates Quantum Efficiency (η), and Quantum Yield (q)

EuMAI	Ω_2	Ω_4	Ω_6	t (ms)	A_{rad} (s^{-1})	A_{nrad} (s^{-1})	η (%)	q (%)
experimental	3.19	3.87	-	0.13	202.7	8131.0	2.40	>1.00
theoretical[a]	3.22	3.80	0.32	-	204.9	8128.5	2.46	0.08

[a]Values derived from the optimized Sparkle/PM3 model.[63]

$$n_w = 1.11 \cdot (A_{tot} - A_{rad} - 0.31) \quad (1)$$

Application of Horrocks rule to **EuMAI** leads to $n_w = 8$. On the basis of all spectroscopic and spectrometric evidence, the structures of the complex and its dissociation in aqueous solution were also optimized via Sparkle/PM3[63] (Figure 3).

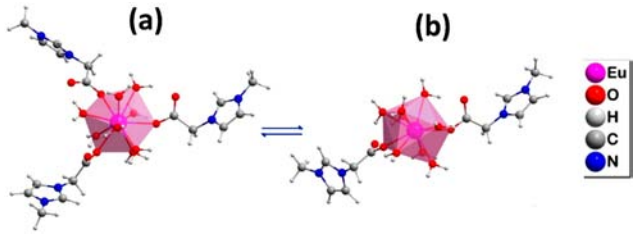

Figure 3. Optimized structure of **EuMAI** and its dissociation in aqueous solution calculated at Spakle/PM3. Two main species found in solution (equilibrium) bearing three ligands (a) and two ligands (b) were optimized. Note that the calculated structures are in accordance with data obtained by NMR and ESI-MS as well as photophysical data.

Theoretical structures of **EuMAI** species presented the Eu^{3+} ions coordinated with 11 oxygen atoms, 3 and 2 of which arise from the **MAI** ligands (Figure 3), and the coordination spheres are completed by aqua ligands; hence, the coordination symmetry of the Ln^{3+} center may be described as a distorted monocapped pentagonal antiprism. The bond lengths among Eu^{3+} ions and **MAI** ligands are shorter than those of Eu^{3+} and aqua ligands, due to the negative charge on the carboxylate oxygen atoms which may increase the binding to the metal center. It is important to note that Figure 3b shows the **MAI** ligands in opposite position to each other, therefore justifying the centrosymmetric profile of the emission spectrum. Tables 1 and 2 show the values for the spectroscopic properties and energy transfer rates calculated for **EuMAI**, respectively.

The calculated values exhibited in Table 1 are in good agreement with those obtained experimentally, evidencing the accuracy of the theoretical methodology.[64] The intramolecular energy transfer, back transfer, and quantum yield of emission for **EuMAI** were calculated considering that the Eu^{3+} levels arise from the metal ion at an intermediate coupling, the energy of the ligand singlet state must be lower than 40.000 cm^{-1}, and the triplet level of the lowest energy must be related to the singlet state previously chosen. Values of energy transfer rates exhibited in Table 2 indicate that the energy transfer occurred from the triplet state (from the ligand) to the $^5D_1$ and $^5D_0$ levels of the Eu^{3+} ion. It is possible to note that the R_L values, that is, the distance from the donor state located at the organic ligands and the Eu^{3+} ion nucleus, are a bit higher. Values down to 5.0 contributed for optimizing the energy transfer rates. Moreover, in both cases the back transfer rates were very high, mainly for **EuMAI**. This fact strongly contributed to a quencher effect for the $^5D_0$ emitter state. All this evidence suggested that vibronic coupling of the O–H oscillators from the aqua ligands and the triplet $^5D_{1,0}$ resonance acted as efficient nonradiative channels for Eu^{3+} emission, thus providing a plausible

dx.doi.org/10.1021/ic4017678 | Inorg. Chem. 2013, 52, 10199–10205

Table 2. Calculated Values of Intramolecular Energy Transfer and Back-Transfer Rates for EuMAI[a]

	ligand state (cm^{-1})		4f state (cm^{-1})	R_L (Å)	transfer rate (s^{-1})	back-transfer rate (s^{-1})
EuMAI Sparkle/PM3 Structure	singlet (37325.3)	→	$^5D_4$ (27586)	7.12	4.30×10^1	2.14×10^{-19}
	triplet (17582.2)	→	$^5D_1$ (19027)	7.24	3.15×10^9	4.03×10^{12}
	triplet (17582.2)	→	$^5D_0$ (17293)	7.24	6.97×10^9	1.79×10^9

[a]The R_L value is the distance from the donor state located at the organic ligands and the Eu^{3+} ion nucleus.

explanation for the short lifetime and low experimental quantum yields. The high values of A_{nrad} are in accordance with this fact (see Table 1).

The Tb^{3+} ions showed moderately influenced transitions by the symmetry of the ligand environment; however, those transitions combine induced electric dipole (ED) and magnetic dipole (MD) characters and no isolated MD transition like those of the Eu^{3+} ions. Therefore, this experiment is difficult due to the complex J degeneracy of the emitting levels of the Tb^{3+}, preventing a wide spectroscopic investigation such as that performed for Eu^{3+} ions. The emission spectrum of **TbMAI** (see Figure 2) acquired at room temperature displayed the typical green Tb^{3+} emission associated with the $^5D_4 \rightarrow {}^7F_J$ transitions. The $^5D_4 \rightarrow {}^7F_5$ transition centered at ca. 542 nm is the strongest one and corresponds to ca. 30% of the integrated emission spectrum. **TbMAI** showed a quantum yield of emission of 17% and a short lifetime (τ) of 0.40 ms. It may be justified by the contributions of O−H oscillators and due to the calculated triplet level to be below the Tb $^5D_4$ emitter state. Previous reports have demonstrated that when the energy difference between the lowest triplet state of the ligand is lower than about 2000 cm^{-1}, the thermal back transfer plays an important role for photoluminescence quenching.[65]

Finally, both complexes were tested as probes in bioimaging experiments to stain MDA-MB-231 cancer cells. First, it is noted that both complexes were capable of transposing the cell membrane, and no precipitation could be noted during the cellular experiments, which are highly desired features. The MDA-MB-231 cells stained with **EuMAI** showed a slight red fluorescence signal with a distribution pattern (Figure 4) closely related with the fluorescence pattern observed with the samples incubated with **TbMAI** (discussed below). The fluorescent signal of **EuMAI** on MDA-MB-231 cells showed a minor association with a perinuclear region plus a homogeneous stain through the cell cytoplasm. The Eu^{3+}-based compound also shows no fluorescent signal related with the cell's nucleus region; therefore, there is no affinity for DNA or others nuclear molecules, even after cell permeabilization procedures. Experiments with **EuMAI** show that this complex is not a good candidate for bioimaging because of its low fluorescence intensity inside the cells. Indeed, this quenching effect in the aqueous cellular environment could be expected, as already depicted from the photophysical data.

The MDA-MB-231 cells stained with **TbMAI**, however, showed an intense and a bright green fluorescence pattern associated with a wide perinuclear region plus homogeneous staining through the cell cytoplasm (Figure 5), therefore contrasting with the fluorescence intensity observed for **EuMAI**. Interestingly, the wide perinuclear region that shows a strong stain pattern (bright green) can be associated with endoplasmic reticulum, as compared with the common pattern observed for this organelle.[66] Indeed, probes capable of exclusive selection of the endoplasmic reticulum in the highly complex cellular environment are very difficult to design, therefore making their planning and synthesis a hard task.[67]

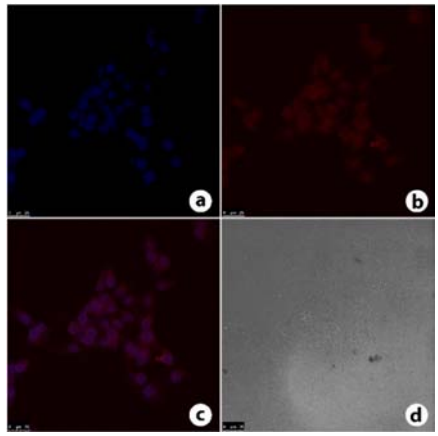

Figure 4. MDA-MB-231 cells. (a) Sample stained only with DAPI (blue). (b) Fluorescence pattern of **EuMAI** with minor association with the perinuclear region plus a homogeneous staining through the cell cytoplasm (red). Samples stained with **EuMAI** show no red fluorescent signal over the nucleus region. (c) Overlay image between a and b. (d) Phase contrast image of MDA-MB-231 cells with normal morphological aspects. Importantly, the red fluorescence emission of **EuMAI** showed herein was artificially slightly improved to facilitate visualization, and it does not represent the actual staining (color intensity) observed for this derivative.

TbMAI also showed no fluorescent signal associated with the cell's nucleus region. This feature demonstrated, by exclusion, no affinity of **TbMAI** with DNA or others nuclear structures such as histone basic proteins, even after cell permeabilization procedures, which would improve the chances of **TbMAI** to get inside of the cell nucleus. **TbMAI** showed a bright green fluorescent signal that persisted for all analysis time periods without fading off, hence making **TbMAI** an outstanding probe for bioimaging experiments to stain endoplasmic reticulum selectively.

EXPERIMENTAL SECTION

The detailed procedure for the syntheses of LnMAI (Ln = Eu^{3+}, Tb^{3+}) derivatives, NMR and high-resolution ESI-MS spectra, and fluorescence lifetime decay procedures are available in the Supporting Information.

CONCLUSION

Fluorescent lanthanide complexes based on the TSIL **MAI·Cl** constitute an attractive class of water-soluble compounds with high potential to be applied as a new family of molecular probes for bioimaging application. In this work, we performed a design of optical bioprobes based on hydrophilic TSIL as ligands and lanthanide ions for cell imaging. NMR spectra and ESI(+)-MS(/MS) provide strong evidence of the equilibrium among distinct lanthanide species in solution. In fact, substitution of one **MAI** ligand directly coordinated to Ln^{3+} ions by water molecules was favored in more dilute solutions. **TbMAI** displayed a green emission and lifetime of 0.40 ms when

dx.doi.org/10.1021/ic4017678 | Inorg. Chem. 2013, 52, 10199−10205

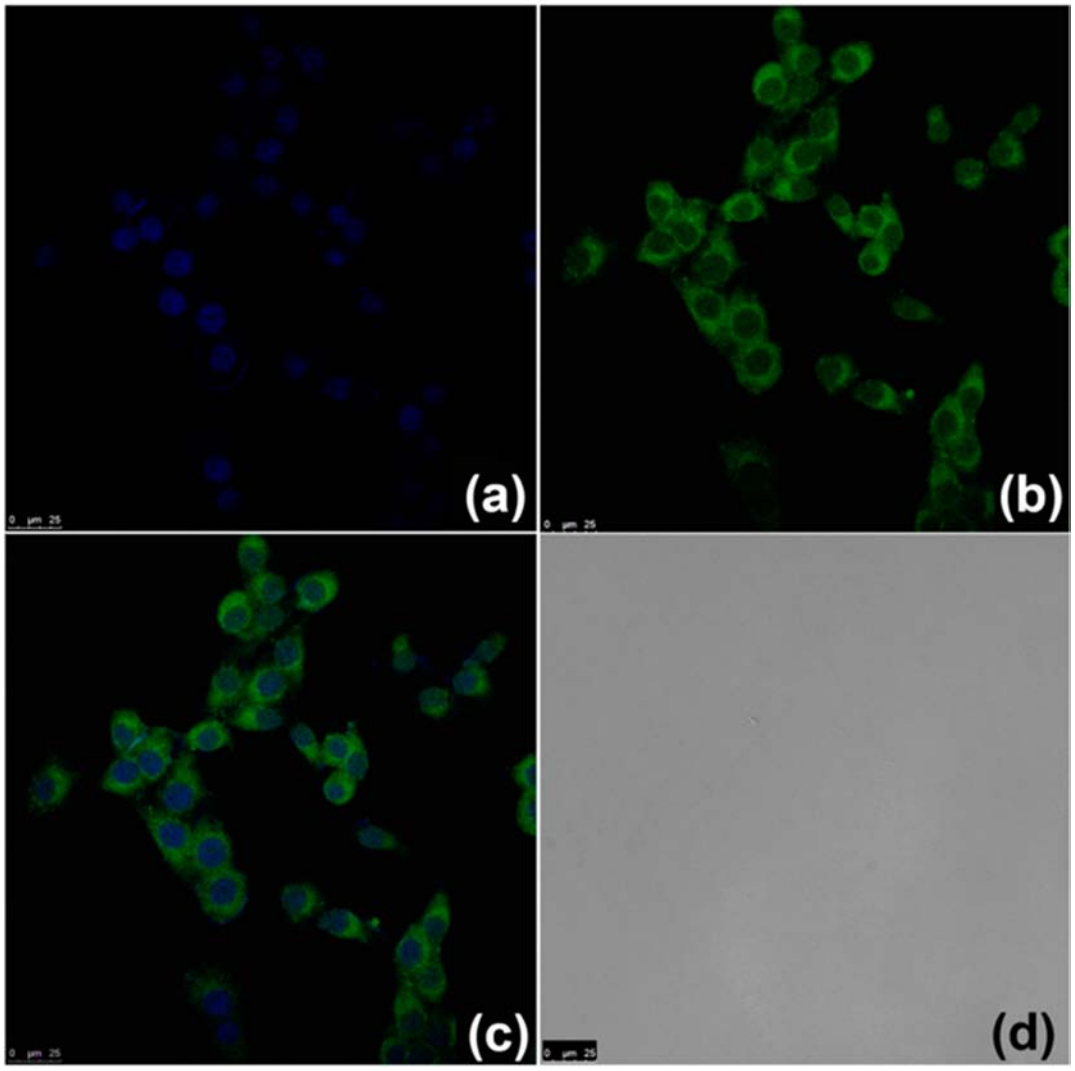

Figure 5. MDA-MB-231 cells. (a) Sample stained only with DAPI (blue). (b) Fluorescence pattern of **TbMAI** slightly associated with the perinuclear region plus a minor homogeneous staining through the cell cytoplasm (green). Further significant feature observed in b was no green staining over the nucleus region on the samples stained with **TbMAI**. (c) Overlay image between DAPI and **TbMAI**. (d) Phase contrast image of MDA-MB-231 cells with normal morphological aspects. Bright green fluorescence emission of **TbMAI** showed herein is the actual staining observed for this derivative.

excited at 367 nm. The coordination geometries, intensity parameters, and energy transfer rates for **EuMAI** were also calculated using Sparkle/PM3. Theoretical intensity parameters, quantum efficiencies, and quantum yields are in good agreement with experimental ones, clearly attesting to the efficacy of the theoretical methodologies. Both complexes were applied as molecular probes in cellular imaging experiments using MDA-MB-231 cells lineage. The good dispensability and prominent luminescent properties presented by **TbMAI** complex make it a molecular probe for further bioimaging experiments. Furthermore, its selectivity toward the endoplasmic reticulum opens up a new avenue for rational design of novel selective fluorescent bioprobes based on the strategy described herein.

■ ASSOCIATED CONTENT

Supporting Information

Experimental procedures, NMR spectra, ESI(+)-MS(/MS) analyses, lifetime decay curves. This material is available free of charge via the Internet at http://pubs.acs.org.

■ AUTHOR INFORMATION

Corresponding Author

*E-mail: marcelozohio@unb.br (M.O.R.); brenno.ipi@gmail.com (B.A.D.N.).

Notes

The authors declare no competing financial interest.

■ ACKNOWLEDGMENTS

The authors gratefully acknowledge CAPES, FAPDF, FINATEC, CNPq (INCT-Inami and INCT-Catalysis), FACEPE (APT-0859-1.06/08), FAPITEC-SE, and DPP-UnB for partial financial support. M.O.R. is also indebted to Leonis L. Luz.

■ REFERENCES

(1) Plechkova, N. V.; Seddon, K. R. *Chem. Soc. Rev.* **2008**, *37*, 123–150.
(2) Feroci, M.; Chiarotto, I.; Inesi, A. *Curr. Org. Chem.* **2013**, *17*, 204–219.
(3) Prediger, P.; Genisson, Y.; Correia, C. R. D. *Curr. Org. Chem.* **2013**, *17*, 238–256.

(4) Dupont, J.; Eberlin, M. N. *Curr. Org. Chem.* **2013**, *17*, 257−272.
(5) Prechtl, M. H. G.; Sahler, S. *Curr. Org. Chem.* **2013**, *17*, 220−228.
(6) Suarez, P. A. Z.; Ramalho, H. F. *Curr. Org. Chem.* **2013**, *17*, 229−237.
(7) Dupont, J.; Meneghetti, M. R. *Curr. Opin. Colloid Interface Sci.* **2013**, *18*, 54−60.
(8) Scholten, J. D.; Leal, B. C.; Dupont, J. *ACS Catal.* **2012**, *2*, 184−200.
(9) Sebesta, R.; Kmentova, I.; Toma, S. *Green Chem.* **2008**, *10*, 484−496.
(10) Lombardo, M.; Trombini, C. *ChemCatChem* **2010**, *2*, 135−145.
(11) Tang, S. K.; Baker, G. A.; Zhao, H. *Chem. Soc. Rev.* **2012**, *41*, 4030−4066.
(12) Chaturvedi, D. *Curr. Org. Chem.* **2011**, *15*, 1236−1248.
(13) Olivier-Bourbigou, H.; Magna, L.; Morvan, D. *Appl. Catal. A: Gen.* **2010**, *373*, 1−56.
(14) Dupont, J.; de Souza, R. F.; Suarez, P. A. Z. *Chem. Rev.* **2002**, *102*, 3667−3691.
(15) Dupont, J.; Scholten, J. D. *Chem. Soc. Rev.* **2010**, *39*, 1780−1804.
(16) Dupont, J. *Acc. Chem. Res.* **2011**, *44*, 1223−1231.
(17) Weingartner, H.; Cabrele, C.; Herrmann, C. *Phys. Chem. Chem. Phys.* **2012**, *14*, 415−426.
(18) Consorti, C. S.; Aydos, G. L. P.; Ebeling, G.; Dupont, J. *Org. Lett.* **2008**, *10*, 237−240.
(19) Lee, S. G. *Chem. Commun.* **2006**, 1049−1063.
(20) Consorti, C. S.; Aydos, G. L. P.; Ebeling, G. *Organometallics* **2009**, *28*, 4527−4533.
(21) Consorti, C. S.; Aydos, G. L. P.; Ebeling, G.; Dupont, J. *Appl. Catal. A: Gen.* **2009**, *371*, 114−120.
(22) Hallett, J. P.; Welton, T. *Chem. Rev.* **2011**, *111*, 3508−3576.
(23) Neto, B. A. D.; Correa, J. R.; Silva, R. G. *RSC Adv.* **2013**, *3*, 5291−5301.
(24) Chen, Y. G.; Guo, W. H.; Ye, Z. Q.; Wang, G. L.; Yuan, J. L. *Chem. Commun.* **2011**, *47*, 6266−6268.
(25) Endres, P. J.; MacRenaris, K. W.; Vogt, S.; Meade, T. J. *Bioconjugate Chem.* **2008**, *19*, 2049−2059.
(26) Deiters, E.; Song, B.; Chauvin, A. S.; Vandevyver, C. D. B.; Gumy, F.; Bunzli, J. C. G. *Chem.—Eur. J.* **2009**, *15*, 885−900.
(27) Steemers, F. J.; Meuris, H. G.; Verboom, W.; Reinhoudt, D. N.; vanderTol, E. B.; Verhoeven, J. W. *J. Org. Chem.* **1997**, *62*, 4229−4235.
(28) Zhou, J.; Zhu, X. J.; Chen, M.; Sun, Y.; Li, F. Y. *Biomaterials* **2012**, *33*, 6201−6210.
(29) Pal, R.; Parker, D. *Org. Biomol. Chem.* **2008**, *6*, 1020−1033.
(30) Guo, D. L.; Chen, T.; Ye, D. J.; Xu, J. Y.; Jiang, H. L.; Chen, K. X.; Wang, H.; Liu, H. *Org. Lett.* **2011**, *13*, 2884−2887.
(31) Nadler, A.; Schultz, C. *Angew. Chem., Int. Ed.* **2013**, *52*, 2408−2410.
(32) Hu, Z. J.; Tian, X. H.; Zhao, X. H.; Wang, P.; Zhang, Q.; Sun, P. P.; Wu, J. Y.; Yang, J. X.; Tian, Y. P. *Chem. Commun.* **2011**, *47*, 12467−12469.
(33) Wong, K.-L.; Law, G.-L.; Murphy, M. B.; Tanner, P. A.; Wong, W.-T.; Lam, P. K.-S.; Lam, M. H.-W. *Inorg. Chem.* **2008**, *47*, 5190−5196.
(34) Palmer, R. J.; Butenhoff, J. L.; Stevens, J. B. *Environ. Res.* **1987**, *43*, 142−156.
(35) de Bettencourt-Dias, A.; Barber, P. S.; Bauer, S. *J. Am. Chem. Soc.* **2012**, *134*, 6987−6994.
(36) Zhao, Q.; Huang, C. H.; Li, F. Y. *Chem. Soc. Rev.* **2011**, *40*, 2508−2524.
(37) Bunzli, J. C. G.; Piguet, C. *Chem. Soc. Rev.* **2005**, *34*, 1048−1077.
(38) Bunzli, J. C. G. *Chem. Rev.* **2010**, *110*, 2729−2755.
(39) Bunzli, J. C. G. *Chem. Lett.* **2009**, *38*, 104−109.
(40) Bunzli, J. C. G.; Comby, S.; Chauvin, A. S.; Vandevyver, C. D. B. *J. Rare Earths* **2007**, *25*, 257−274.
(41) Li, H. R.; Shao, H. F.; Wang, Y. G.; Qin, D. S.; Liu, B. Y.; Zhang, W. J.; Yan, W. D. *Chem. Commun.* **2008**, 5209−5211.
(42) Feng, J.; Zhang, H. J. *Chem. Soc. Rev.* **2013**, *42*, 387−410.
(43) Eliseeva, S. V.; Bunzli, J. C. G. *Chem. Soc. Rev.* **2010**, *39*, 189−227.
(44) Binnemans, K. *Chem. Rev.* **2007**, *107*, 2592−2614.
(45) Wen, T. T.; Li, H. R.; Wang, Y. G.; Wang, L. Y.; Zhang, W. J.; Zhang, L. *J. Mater. Chem. C* **2013**, *1*, 1607−1612.
(46) Dupont, J.; Suarez, P. A. Z. *Phys. Chem. Chem. Phys.* **2006**, *8*, 2441−2452.
(47) Neto, B. A. D.; Carvalho, P. H. P. R.; Santos, D. C. B. D.; Gatto, C. C.; Ramos, L. M.; de Vasconcelos, N. M.; Corrêa, J. R.; Costa, M. B.; de Oliveira, H. C. B.; Silva, R. G. *RSC Adv.* **2012**, *2*, 1524−1532.
(48) Oliveira, F. F. D.; Santos, D.; Lapis, A. A. M.; Correa, J. R.; Gomes, A. F.; Gozzo, F. C.; Moreira, P. F.; de Oliveira, V. C.; Quina, F. H.; Neto, B. A. D. *Bioorg. Med. Chem. Lett.* **2010**, *20*, 6001−6007.
(49) Alvim, H. G. O.; Fagg, E. L.; de Oliveira, A. L.; de Oliveira, H. C. B.; Freitas, S. M.; Xavier, M.-A. E.; Soares, T. A.; Gomes, A. F.; Gozzo, F. C.; Silva, W. A.; Neto, B. A. D. *Org. Biomol. Chem.* **2013**, *11*, 4764−4777.
(50) Weber, I. T.; de Melo, A. J. G.; Lucena, M. A. D.; Rodrigues, M. O.; Alves, S. *Anal. Chem.* **2011**, *83*, 4720−4723.
(51) Weber, I. T.; Terra, I. A. A.; de Melo, A. J. G.; Lucena, M. A. D.; Wanderley, K. A.; Paiva-Santos, C. D.; Antonio, S. G.; Nunes, L. A. O.; Paz, F. A. A.; de Sa, G. F.; Junior, S. A.; Rodrigues, M. O. *RSC Adv.* **2012**, *2*, 3083−3087.
(52) Rodrigues, M. O.; Dutra, J. D. L.; Nunes, L. A. O.; de Sa, G. F.; de Azevedo, W. M.; Silva, P.; Paz, F. A. A.; Freire, R. O.; Junior, S. A. *J. Phys. Chem. C* **2012**, *116*, 19951−19957.
(53) Oliveira, F. F. D.; dos Santos, M. R.; Lalli, P. M.; Schmidt, E. M.; Bakuzis, P.; Lapis, A. A. M.; Monteiro, A. L.; Eberlin, M. N.; Neto, B. A. D. *J. Org. Chem.* **2011**, *76*, 10140−10147.
(54) Binnemans, K. *Chem. Rev.* **2009**, *109*, 4283−4374.
(55) Kirby, A. F.; Foster, D.; Richardson, F. S. *Chem. Phys. Lett.* **1983**, *95*, 507−512.
(56) Tiseanu, C.; Parvulescu, V. I.; Kumke, M. U.; Dobroiu, S.; Gessner, A.; Simon, S. *J. Phys. Chem. C* **2009**, *113*, 5784−5791.
(57) Coelho, F.; Eberlin, M. N. *Angew. Chem., Int. Ed.* **2011**, *50*, 5261−5263.
(58) Borges, A. S.; Dutra, J. D. L.; Freire, R. O.; Moura, R. T.; Da Silva, J. G.; Malta, O. L.; Araujo, M. H.; Brito, H. F. *Inorg. Chem.* **2012**, *51*, 12867−12878.
(59) dos Santos, E. R.; Freire, R. O.; da Costa, N. B.; Paz, F. A. A.; de Simone, C. A.; Júnior, S. A.; Araújo, A. A. S.; Nunes, L. A. n. O.; de Mesquita, M. E.; Rodrigues, M. O. *J. Phys. Chem. A* **2010**, *114*, 7928−7936.
(60) Rodrigues, M. O.; Paz, F. A.; Freire, R. O.; de Sa, G. F.; Galembeck, A.; Montenegro, M. C.; Araujo, A. N.; Alves, S. *J. Phys. Chem. B* **2009**, *113*, 12181−12188.
(61) Liu, F. Y.; Roces, L.; Ferreira, R. A. S.; Garcia-Granda, S.; Garcia, J. R.; Carlos, L. D.; Rocha, J. *J. Mater. Chem.* **2007**, *17*, 3696−3701.
(62) Supkowski, R. M.; Horrocks, W. D., Jr. *Inorg. Chim. Acta* **2002**, *340*, 44−48.
(63) Freire, R. O.; Rocha, G. B.; Simas, A. M. *J. Braz. Chem. Soc.* **2009**, *20*, 1638−1645.
(64) Dutra, J. D. L.; Freire, R. O. *J. Photochem. Photobiol., A* **2013**, *256*, 29−35.
(65) Latva, M.; Takalo, H.; Mukkala, V. M.; Matachescu, C.; RodriguezUbis, J. C.; Kankare, J. *J. Lumin.* **1997**, *75*, 149−169.
(66) Zhong, Y. W.; Fang, S. Y. *J. Biol. Chem.* **2012**, *287*, 28057−28066.
(67) Srikun, D.; Albers, A. E.; Nam, C. I.; Iavaron, A. T.; Chang, C. J. *J. Am. Chem. Soc.* **2010**, *132*, 4455−4465.